Quantitative Relations between Glass Transition Temperatures and Thermodynamic Parameters for Various Materials: Molecular Design for Nonpolymeric Organic Dye Glasses with Thermal Stability

Katsuyuki Naito

Advanced Research Laboratory, Research and Development Center, Toshiba Corporation 1, Komukai Toshiba-cho, Saiwai-ku, Kawasaki 210, Japan

Received May 24, 1994. Revised Manuscript Received October 3, 1994[⊗]

Quantitative relations between amorphous thermal properties and thermodynamic parameters of phase transitions have been investigated to obtain a molecular design rule for uniform dye amorphous films with high thermal stability. A high glass transition temperature (T_g/K), a low maximum crystal-growth velocity (MCV/ms^{-1}), and a high maximum crystal-growth temperature ($T_{c,max}$/K) are required for thermally stable glasses. The following equation has been established semiempirically and confirmed experimentally: $T_g = h_g/(\sum\Delta S_{tr,m}/N)$, where h_g is a material family constant corresponding to the activation energy for heavy atom rearrangement. ($\sum\Delta S_{tr,m}$/J K^{-1} mol^{-1}) means the sum of the entropies of fusion and of phase transitions for a crystalline sample between T_g and the melting point (T_m/K), and N is the number of heavy atoms per molecule or per repeated unit except hydrogen atoms. Higher-network materials give larger h_g values. The following equation has also been established: $MCV = k_0 \exp\{-h_{mc}N/(T_m\sum\Delta H_{tr,m})\}$, where k_0 is a constant and h_{mc} is a material family constant. ($\sum\Delta H_{tr,m}$/kJ mol^{-1}) means the sum of the enthalpies of fusion and of phase transitions between $T_{c,max}$ and T_m. As the network degree increased, h_{mc} increased, resulting in a small MCV. Nonpolymeric poly(hydrogen-bonding) molecules with a large, symmetric, globular, rigid, and dense structure have been newly synthesized to realize large h_g and small $\sum\Delta S_{tr,m}/N$ values, resulting in high-T_g amorphous states (~500 K).

Introduction

Organic dye molecules have attracted much attention due to their various optical and electrical properties.[1] The properties are mainly derived from a π-electron system, which is usually located in a molecule. Electric carriers injected from electrodes or generated by irradiation cannot move freely in their bulk solids. To overcome this disadvantage, thin films of organic dye molecules formed by the Langmuir–Blodgett method[2] and the molecular beam epitaxy method,[3] etc., have recently been investigated.

Optical and/or electric devices using organic thin films controlled by solid electrodes require film homogeneity to avoid undesired electric short circuits, although the device characteristics are substantially affected by various types of carrier traps within the films. Monocrystalline thin films without any structural imperfections are thus considered to be ideal. However, it is very difficult to form monocrystalline thin films of complex organic functional molecules on conventional electrodes with thicknesses less than 100 nm. Moreover, polycrystalline films prepared by conventional methods always have grain boundaries of various sizes, which cause serious structural defects and deep carrier traps. An alternative approach to form uniform organic films is to produce amorphous (glass) thin films.

Many studies have been carried out on glasses including organic materials.[4] However, nonpolymeric organic glasses have been considered to be thermally unstable. Efforts to synthesize amorphous dyes have been made mainly to solve them as much as possible in thermally stable amorphous polymers for xerography or color filters, etc., not to improve their own thermal stabilities.

Organic electroluminescent (EL) devices, however, recently reported by Tang et al.[5] have required such thermal stabilities. The devices were composed of layered dye films of 10–50 nm thicknesses sandwiched between electrodes. The dye layers have usually been constructed by conventional physical vapor deposition, and therefore nonpolymeric amorphous dye compounds

[⊗] Abstract published in *Advance ACS Abstracts,* November 15, 1994.

(1) For example: (a) Ashwell, G. J., Ed. *Molecular Electronics*: Research Studies: 1992. (b) Liu, C.-Y.; Pan, H.-L.; Fox, M. A.; Bard, A. J. *Sicence* **1993**, *261*, 897. Rambidi, N. G.; Chernavskii, D. S.; Sandler, Yu. M. *J. Mol. Electron.* **1991**, *5*, 105. (c) Carter, F. L., Ed. *Molecular Electronic Devices*; Dekker: New York, 1983.

(2) For example: (a) Barraud, A.; Palacin, S., Ed. *Langmuir-Blodgett Films 5: Proceedings of 5th International Conference on Langmuir-Blodgett Films*; Elsevier: Amsterdam, 1991. (b) Roberts, G., Ed. *Langmuir-Blodgett Films*: Plenum: New York, 1990. (c) Adams, N. K. *The Physics and Chemistry of Surfaces*; Dover: New York, 1968. (d) Naito, K.; Mium, A. *Thin Solid Films* **1994**, *242*, 191.

(3) For example: (a) *Mol. Electron. Bioelectron.* **1992**, *3*, 228–282 (Japanese). (b) Möbus, M.; Karl, N. *Thin Solid Films* **1992**, *215*, 213. (c) Zimmerman, U.; Karl, N. *Surf. Sci.* **1992**, *268*, 296. (d) Haskal, E. I.; So, F. F.; Burrows, P. E.; Forrest, S. R. *Appl. Phys. Lett.* **1992**, *60*, 3223.

(4) For example: (a) Ngai, K. L., Wright, G. B. Eds. *Proceedings of the International Discussion Metting on Relaxations in Complex Systems. J. Non-Cryst. Solids* **1990**, *131–133*. (b) Williams, G. *J. Non-Cryst. Solids* **1991**, *131–133*, 1. (c) Schefer, G. W. *J. Non-Cryst. Solids* **1990**, *123*, 75. (d) Yonezawa, F. *Solid State Phys.* **1991**, *45*, 179. (e) Bondi, A. *Physical Properties of Molecular Crystals, Liquids, and Glasses*; John Wiley: New York, 1968; pp 370–449.

(5) (a) Tang, C. W.; VanSlyke, S. A. *Appl. Phys. Lett.* **1987**, *51*, 913. (b) Tang, C. W.; VanSlyke, S. A.; Chen, C. H. *J. Appl. Phys.* **1989**, *65*, 3610.

0897-4756/94/2806-2343$04.50/0

used in the devices must have glass transition temperatures (T_g) at least higher than room temperature. However, their thermal stability is still insufficient. As a result, the layered dye films are frequently damaged during evaporation of the metal electrodes and also while driving the devices at high electric current densities.

The stability of amorphous phases is usually elucidated by the crystal-growth velocity (*CV*), which is a kinetic parameter related to the transition from amorphous to crystalline phases. The crystal-growth velocity is known to be a bell-shaped function of temperature, having a maximum (*MCV*) at $T_{c,max}$ a little lower than the melting point (T_m). High $T_{c,max}$ and low *MCV* are thus required for stable amorphous states of organic materials in addition to the high T_g.

Such needs have given birth to a new concept of nonpolymeric organic dye glasses with thermal stability. The resulting concept is no longer limited to EL devices and can be expected to extend to many fields such as xerography, photocells, memory devices, color filters, etc. It is necessary to control the amorphous thermal properties for these applications. Shirota et al. have synthesized many "star-burst" molecules with a high T_g and have reported thermal and electric properties.[6] Large specific heat changes have been observed at T_g for high T_g compounds as well as for many organic liquids. The relations between their molecular structures and amorphous properties have not yet been well clarified.

In a previous paper,[7] the author and his colleague described the quantitative relations between the amorphous parameters (T_g, *MCV*, $T_{c,max}$) and thermodynamic parameters ($\sum\Delta S_{tr,m}$, $\sum\Delta H_{tr,m}$, T_m) concerned with phase transitions:

$$T_g = a - b\sum\Delta S_{tr,m}/N$$

$$\log(MCV) = c - dN/(T_m\sum\Delta H_{tr,m})$$

where $a-d$ are constants, N is the number of heavy atoms per molecule except hydrogen atoms, $\sum\Delta S_{tr,m}$ means the sum of the entropies of fusion and of phase transitions between T_g and T_m, and $\sum\Delta H_{tr,m}$ is the sum of the enthalpies of fusion and phase transitions between $T_{c,max}$ and T_m. The findings have indicated that it is possible to form heat-resistive and stable nonpolymeric organic dye glasses with high T_g and $T_{c,max}$ and with small *MCV* from large, symmetric, rigid, and dense molecules. Furthermore, the possibility of network molecules has been suggested for improving the amorphous natures.

The present paper shows the results of the author's more precise investigations of the equations and of the trials concluded to extend them as universal equations to various materials, including hydrogen-bonding molecules, polymers, and inorganic materials. According to the results, network molecules with plural hydrogen-bonding sites showing T_g as high as 500 K have been synthesized.

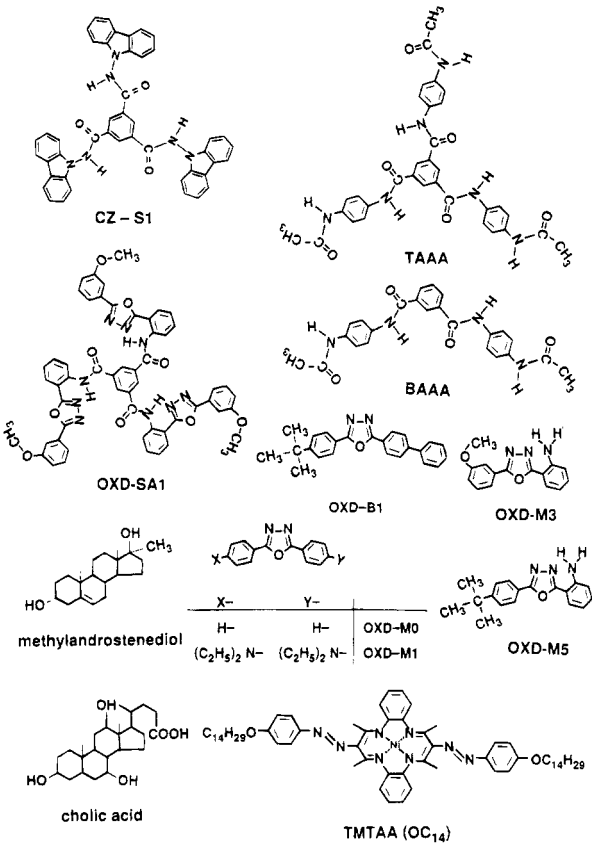

Figure 1. Molecular structures of nonpolymeric organic compounds with high T_g used in this study. Many other molecules were shown in a previous paper.[7]

Experimental Section

Figure 1 shows high-T_g organic compounds used in this study excepting the molecules presented in a previous paper.[7] Reagent grades of steroids were purchased from Tokyo Kasei (Japan) and were used without any purification. The data for the polymers and inorganic materials were taken from literature. The method for measuring the thermal properties has also been described in a previous paper.[7]

CZ-S1 was prepared from 1,3,5-benzenetricarbonyl trichloride (Aldrich) and *N*-aminocarbazole (Shimakyu, Japan) in dry pyridine. Anal. Calcd for $C_{45}H_{30}N_6O_3$: C, 76.7; H, 4.3; N, 11.9. Found: C, 76.0; H, 4.0; N, 11.0. IR (KBr, cm^{-1}) 3300 (b, NH); 3056 (w, PhH); 1705 (s, C=O); 1606 (m, C=C); 1484 (m, amide, carbazole); 1452 (s, carbazole); 1316 (m); 1231 (s); 746 (s); 720 (m). ^1H NMR (DMSO-d_6, ppm) δ 12.1 (s, NH, 3H); 8.8 (b, center Ph−H, 3H); 8.2−7.2 (complex, carbazole, 24H).

OXD-SA1 was prepared from 1,3,5-benzenetricarbonyl trichloride and 5-(2-aminophenyl)-2-(3-methoxyphenyl)-1,3,4-oxadiazole (Maybridge, UK) in dry pyridine. Anal. Calcd for $C_{54}H_{39}N_9O_9$: C, 67.7; H, 4.1; N, 13.2. Found: C, 67.7; H, 4.1; N, 13.4.

BAAA was prepared from 1,3-benzenedicarbonyl dichloride (Aldrich) and 4-aminoacetanilide.[8] ^1H NMR (DMSO-d_6, ppm) δ 10.37 (s, NH, 2H); 9.94 (s, NH, 2H); 8.51 (s, center Ph−H, 1H); 8.12 (q, center Ph−H, 2H); 7.71 (d, Ph−H, J = 9.3 Hz, 4H); 7.67 (d, center Ph−H, J = 7.8 Hz, 1H); 7.57 (d, Ph−H, J = 8.8 Hz, 4H); 2.04 (s, CH_3, 6H).

TAAA was prepared from 1,3,5-benzenetricarbonyl trichloride and 4-aminoacetanilide. ^1H NMR (DMSO-d_6, ppm) δ 10.53 (s, NH, 3H); 9.96 (s, NH, 3H); 8.7 (s, center Ph−H, 3H);

(6) (a) Ishikawa, W.; Inada, H.; Nakano, H.; Shirota, Y. *J. Phys. D: Appl. Phys.* **1993**, *26*, B94. (b) Ishikawa, W.; Noguchi, K.; Kuwabara, Y.; Shirota, Y. *Adv. Mater.* **1993**, *5*, 559. (c) Ishikawa, W.; Inada, H.; Nakano, H.; Shirota, Y. *Mol. Cryst. Liq. Cryst.* **1992**, *211*, 431. (d) Higuchi, A.; Inada, H.; Kobata, T.; Shirota, Y. *Adv. Mater.* **1991**, *3*, 549. (e) Nishimura, K.; Kobata, T.; Inada, H.; Shirota, Y. *J. Mater. Chem.* **1991**, *1*, 897. (f) Shirota, Y.; Kobata, T.; Noma, N. *Chem. Lett.* **1989**, 1145.

(7) Naito, K.; Miura, A. *J. Phys. Chem.* **1993**, *97*, 6240.

(8) Naito, K.; Miura, A.; Azuma, M. *J. Am. Chem. Soc.* **1991**, *113*, 6386.

Table 1. Relation between T_g and Apparent Activation Energy $E_{a,g}$ for Viscous Flow at T_g ($\eta = 10^{13}$ P)

compound	$E_{a,g}$ (kJ/mol)	ref	T_g (K)
trinaphthylbenzene	500	17	342
o-terphenyl	430	10	245
propylene carbonate	250	10	152
$Na_2O{\cdot}2SiO_2$	640	18	732
$Li_2O{\cdot}2SiO_2$	420	19	724
$Na_2O{\cdot}SiO_2$	600	18	683
B_2O_3	380	20	553
As_2O_3	210	21	433
$CaO{\cdot}SiO_2$	1100	22	1065
$Na_2O{\cdot}2B_2O_3$	870	23	753
SiO_2	710	24	1463
GeO_2	310	25	800

7.73 (d, Ph−H, J = 8.8 Hz, 6H); 7.59 (d, Ph−H, J = 8.8 Hz, 6H); 2.05 (s, CH_3, 9H).

Theoretical Approach for Amorphous Properties

T_g and Thermodynamic Parameters. Regarding glass transition, a widely accepted concept is that transition takes place when the viscosity (η) of the relevant supercooled liquid reaches 10^{13} P (=10^{12} N s/m^2).[9] The temperature dependencies of viscosities for various supercooled liquids generally deviate from simple Arrhenius equations. The apparent activation energies (E_a) increase as the temperature decreases. The behaviors are different among material families. E_a does not change very much for three-dimensional network materials like SiO_2 and GeO_2. The temperature dependence of E_a becomes large as the networks are broken down into small molecular liquids. Angell showed Arrhenius plots using a reduced temperature (T/T_g) and indicated that materials in the same family with a similar network property yielded similar curves.[10] Therefore, T_g is proportional to E_a at 10^{13} P for materials in the same family.

To verify this, apparent E_a values at 10^{13} poise ($E_{a,g}$) were obtained from viscosity data for various glass-forming supercooled liquids, as shown in Table 1. Figure 1 indicates the relations between T_g and $E_{a,g}$. As predicted above, T_g is almost proportional to $E_{a,g}$ for materials of the same family.

According to the theory proposed by Adam and Gibbs[11] and to that recently developed by Ngai,[12] a cooperative rearrangement of motional segments is necessary for the viscous flow of a supercooled liquid. The segment unit is considered to be a heavy atom in the present paper. The activation energy for the cooperative rearrangement per unit is described by E_0. E_0 can be almost the same for materials of the same family (i.e., material family constant). The smallest number of units for cooperative rearrangement is expressed by Z^*. So, E_a is equal to E_0Z^*. Z^* increases as T decreases.

The number of possible configurations of a heavy atom is described as W. The entropy of rearrangement for one molar heavy atom (S_c) can be expressed by $k_B(N_A/Z^*)\ln(W)$, where k_B is the Boltzmann constant and N_A is the Avogadro number:

$$E_a = E_0Z^* = E_0k_B(N_A/S_c)\ln(W) = BR/S_c \quad (1)$$

B is equal to $E_0\ln(W)$ and is a material family constant. R is the gas constant. S_c is equal to S_e/N, where S_e is the molar entropy difference between a supercooled liquid and a crystal at T. N is the number of heavy atoms of a molecule or a repeated unit. The viscosity of a supercooled liquid is given by

$$\eta = \eta_0 \exp(E_a/RT) = \eta_0 \exp(BN/(S_eT)) \quad (2)$$

where η_0 has been found to be constant (10^{-4} P) for various materials.[10] Since η is 10^{13} P at T_g, T_g can be expressed by

$$T_g = 0.026BN/S_g \quad (3)$$

where S_g is S_e at T_g. S_g can be exactly described by

$$S_g = \sum\Delta S_{tr,m} - \int_{T_g}^{T_m}\Delta C_P/T\,dT \quad (4)$$

where $\sum\Delta S_{tr,m}$ is the sum of the entropies of fusion and of phase transitions between T_g and T_m. ΔC_P is the specific heat difference between a supercooled liquid and a crystal. By assuming that ΔC_P is a constant between T_g and T_m, eq 5 is established:

$$S_g = \sum\Delta S_{tr,m} - \Delta C_P\ln(T_m/T_g) \quad (5)$$

For glass-forming materials, T_m/T_g is known to be almost constant ($^3/_2$).[13] Both $\sum\Delta S_{tr,m}$ and ΔC_P are based on the difference of the configuration numbers for heavy atoms between a liquid and a crystal. Therefore, S_g can be approximated by

$$S_g = D\sum\Delta S_{tr,m} \quad (6)$$

where D is a material family constant. D is near 0.5 for non(hydrogen-bonding) aromatic compounds, and larger for 3-dimensional network-forming materials like GeO_2. From eqs 3 and 6, eq 7 has been established,

$$T_g = (0.026B/D)N/\sum\Delta S_{tr,m} = h_g/(\sum\Delta S_{tr,m}/N) \quad (7)$$

where h_g is a material family constant, corresponding to $E_0\ln(W)/D$. E_0 can be considered to increase as the network degree increases. h_g is large for network-forming materials.

In the above theoretical approach, $\sum\Delta S_{tr,m}/N \rightarrow 0$ indicates Z^* and $E_a \rightarrow \infty$. This means that atoms in a crystal cannot rearrange at all. However, diffusion and dislocation of atoms take place in a crystal at high temperatures. In practice, this deviation can be considered to decrease the h_g value in a small $\sum\Delta S_{tr,m}$ region.

The viscosity at T_g measured by DSC is known to be smaller than 10^{13} P.[44] For high-T_g inorganic glasses it is typically about 10^{12} P. For low-T_g inorganic glasses and for organic glasses and polymers it is about 10^{10} P. Therefore, the value of 0.026 in eq 3 changes a little in

(9) Bondi, A. *Physical Properties of Molecular Crystals, Liquids, and Glasses*; John Wiley: New York, 1968; p 372.
(10) Angell, C. A. *J. Phys. Chem. Solids* **1988**, *49*, 863.
(11) Adam, G.; Gibbs, J. H. *J. Chem. Phys.* **1965**, *43*, 139.
(12) Ngai, K. L. *J. Non-Cryst. Solids* **1991**, *131−133*, 80.
(13) (a) Kauzmann, W. *Chem. Rev.* **1948**, *43*, 219. (b) Beaman, R. G. *J. Polym. Sci.* **1952**, *9*, 470. (c) Sakka. S.; Mackenzie, J. D. *J. Non-Cryst. Solid* **1971**, *6*, 145.

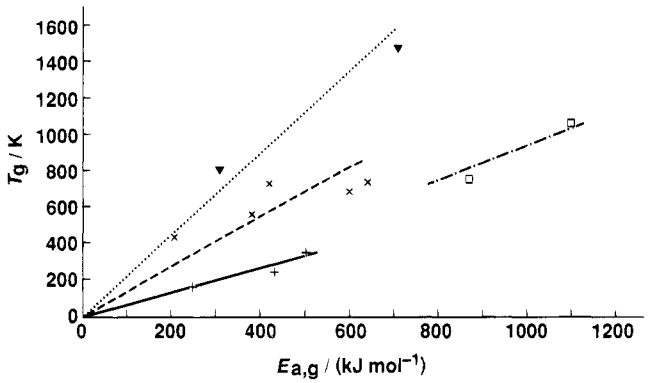

Figure 2. Relation between glass transition temperature (T_g) and apparent activation energy ($E_{a,g}$) for viscosity of supercooled liquids at T_g for non(hydrogen-bonding) molecules (+), for low network inorganic materials such as B_2O_3, As_2O_3, $Na_2O{\cdot}SiO_2$ (×), for moderate network inorganic materials such as $Na_2O{\cdot}2B_2O_3$ (□), and for high network inorganic materials such as SiO_2 and GeO_2 (▼). See Table 1.

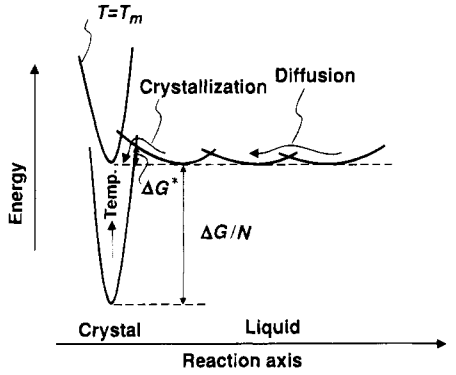

Figure 3. Schematic explanation for crystallization of supercooled liquids. Motional segment units diffuse in a supercooled liquid and then crystallize at a crystal/liquid interface. The potential barrier (ΔG^*) of crystallization decreases with temperature decrement, because a free energy difference ($\Delta G/N$) between a crystal and a supercooled liquid increases.

different material families: 0.027 for 10^{12} P and 0.031 for 10^{10} P. Equation 7 can be also established in these cases.

Maximum Crystal-Growth Velocity (*MCV*) and Thermodynamic Parameters. The quantitative equation for non(hydrogen-bonding) aromatic compounds has been obtained in a previous paper.[7] In the present paper, the author has tried to apply the equation to other glass-forming materials.

It is known that crystal-growth in a supercooled liquid involves two processes, as shown in Figure 3: one is molecular diffusion in a bulk liquid and the other is crystallization at the crystal/liquid interface.[14] The diffusion process is predominant at low temperatures, while the latter prevails at high temperatures. $T_{c,max}$ appears near T_m for various materials according to data in previous studies shown in Table 7 and is described by

$$T_{c,max} = fT_m \tag{8}$$

where f is a constant (=0.94 ± 0.04). Therefore, *MCV* is determined primarily by the crystallization at the interface. The following equations have been obtained

(14) (a) van Hook, A. *Crystallization*; Reinhold: New York, 1961; p 138. (b) Volmer, M.; Marder, M. Z. *Z. Phys. Chem.* **1931**, *154A*, 97.

Table 2. Relation between T_g and Transition–Fusion Entropies for Aromatic Compounds[a]

compound	T_m (K)	T_g (K)	ref	$\sum\Delta S_{tr,m}/N$ (J/K mol)	ref
OXD-S1	541	412	7	0.67[b]	7
TMTAA(OC_{14})	398	336	26	3.00[c]	26
OXD-M1	423	303	tw	2.77[d]	tw
OXD-B1	408	294	tw	2.52	tw
OXD-N1	453	290	tw	3.06	tw
OXD-M5	451	294	tw	2.73	tw
OXD-M3	392	276	tw	3.56	tw

[a] Many other data were shown in a previous paper.[7] [b] Data for T_m and $\sum\Delta S_{tr,m}/N$ were corrected. [c] T_{tr} = 395 K, ΔH = 86.6 kJ/mol. [d] T_{tr} = 386 K, ΔH = 5.72 kJ/mol.

Table 3. Relation between T_g and Transition–Fusion Entropies for Poly(hydrogen-bonding) Compounds

compound	T_m (K)	T_g (K)	ref	$\sum\Delta S_{tr,m}/N$ (J/K mol)	ref.
CZ-S1	n.o.[a]	500	tw		tw
TAAA	630	468	tw	3.34	tw
BAAA	633	404	tw	3.53	tw
OXD-SA1	581	403	tw	1.89	tw
cholic acid	470	388	tw	3.01	tw
methylandrostenediol	477	344	tw	3.7	tw
glucose	414	290	7	6.67	7
$Mg(OAc)_2{\cdot}4H_2O$	333	270	27	9.7	27
resolucinol	383	240	7	7.6	7
$Ca(NO_3)_2{\cdot}4H_2O$	316	217	27	5.8	27
$Cd(NO_3)_2{\cdot}4H_2O$	323	213	27	7.6	27
glycerol	292	186	7	10.5	7
$H_2SO_4{\cdot}3H_2O$	237	158	27	12.8	27
ethanediol	260	152	7	10.8	7
water	273	135	7	22.0	7

[a] Decomposed before melting.

according to a similar discussion described in a previous paper:[7]

$$\Delta G^* \approx A/(\Delta G/N) \tag{9}$$

$$\Delta G = \sum\Delta H_{tr,m}(T_m - T_{c,max})/T_m \tag{10}$$

$$MCV = k_0 \exp(-\Delta G^*/RT_{c,max}) \tag{11}$$

From eqs 8–11

$$MCV = k_0 \exp\{-h_{mc}N/(T_m\sum\Delta H_{tr,m})\} \tag{12}$$

where k_0 is a constant. h_{mc} is a material family constant equal to $A/\{Rf(1-f)\}$. $\sum\Delta H_{tr,m}$ means the sum of the enthalpies of fusion and of phase transitions between $T_{c,max}$ and T_m.

In Figure 3, the potential curves of a supercooled liquid can be considered steeper for network-forming materials than those for nonaggregating materials. Steep curves yield large A and large h_{mc} values.

In the present paper, eqs 7 and 12 are available only for one-component glasses. This is because that the $\sum\Delta S_{tr,m}$ and $\sum\Delta H_{tr,m}$ terms do not include any contribution from mixing of glass-forming materials. For multicomponent systems, further investigation is necessary.

Experimental Results and Discussion

Glass Transition Temperature (T_g). Tables 2–6 indicate the numerical data for various materials. Many data for aromatic and aliphatic compounds have already been shown in a previous paper.[7] In this paper, data for other materials are listed in the tables.

Figure 4 shows the relations between T_g and $\sum\Delta S_{tr,m}/N$ for aromatic, aliphatic, and poly(hydrogen-bonding)

Table 4. Relation between T_g and Transition–Fusion Entropies for Non(hydrogen-bonding) Polymers

materials	T_g (K)	ref[a]	$\Sigma\Delta S_{tr,m}/N$ (J/K mol)	ref[a]
poly(2,6-dimethyl-1,4-phenylene oxide)	480		1.06	
poly(2,6-dimethoxy-1,4-phenylene oxide)	433		0.53	
poly(4,4′-dioxydiphenyl-2,2-propane)carbonate	415		3.48	
isotactic polystyrene	364		2.06	
poly(ethylene terephthalate)	342		2.40	
poly(4-methylpentene-1)	303		3.27	
syndiotactic polypropylene	267		4.23	
poly(octamethylene oxide)	260		9.09	
isotactic polypropylene	259		5.91	
poly(1-butene)	249		3.41	
sulfur(rhombic)	245	28	5.50[b]	29
poly(ethylene adipate)	230		5.11	
poly(ethylene oxide)	220		9.11	
polydioxane	209		9.48	
natural rubber	201		2.92	
poly(propylene oxide)	201		5.37	
poly(oxacyclobutane)	196		7.74	
polydioxepane	189			
poly(tetramethylene oxide)	187		8.65	
trans-polypentenamer	175			
cis-1,4-polybutadiene	165		8.26	
cis-polypentenamer	158			
poly(dimethylsiloxane)	150		4.78	

[a] All data were taken from ref 27. [b] T_{tr} = 369 K, ΔH = 0.40 kJ/mol.

Table 5. Relation between T_g and Transition–Fusion Entropies for Poly(hydrogen-bonding) Polymers[a]

materials	T_g (K)	$\Sigma\Delta S_{tr,m}/N$ (J/K mol)
nylon-6	325	5.01
polyglycolide	318	
polyurethane from HMDI[b] and diethylene glycol	275	4.40
polyurethane from HMDI and triethylene glycol	267	4.89
polyurethane from HMDI and tetraethylene glycol	253	4.93
polyurethane from HMDI and hexaethylene glycol	240	5.37

[a] All data were taken from ref 27. [b] Hexamethylene diisocyanate.

Table 6. Relation between T_g and Transition–Fusion Entropies for Various Inorganic Materials

materials	T_m (K)	T_g (K)	ref	$\Sigma\Delta S_{tr,m}/N$ (J/K mol)	ref
$Li_2O{\cdot}2SiO_2$	1307	724	30	4.7[a]	29
$Na_2O{\cdot}2SiO_2$	1142	732	28	3.6[b]	29
$Na_2O{\cdot}SiO_2$	1362	683	31	6.3	29
B_2O_3	723	553	28	6.6	29
P_2O_5	693	537	28	5.6	35
As_2O_3 (arsenolite)	582	433	28	7.3	29
selenium	493	305	28	12.8[c]	29
$Li_2O{\cdot}2B_2O_3$	1190	753	32	7.8	29
$Na_2O{\cdot}2B_2O_3$	1016	753	33	6.1	29
$K_2O{\cdot}2B_2O_3$	1140	680	28	7.1	29
$CaO{\cdot}SiO_2$	1817	1065	34	7.1[d]	29
$MgO{\cdot}SiO_2$	1830	1063	34	8.5[e]	29
SiO_2 cristobalite, high	1996	1463	28	1.7[f]	29
GeO_2	1388	800	28	11.0	29

[a] T_{tr} = 1209 K, ΔH = 0.94 kJ/mol. [b] T_{tr1} = 951 K, ΔH = 0.42 kJ/mol, T_{tr2} = 980 K, ΔH = 0.63 kJ/mol. [c] T_{tr} = 423 K, ΔH = 0.75 kJ/mol. [d] T_{tr} = 1463 K, ΔH = 7.1 kJ/mol. [e] T_{tr} = 1258 K, ΔH = 1.63 kJ/mol. [f] T_{tr} = 1743 K, ΔH = 0.21 kJ/mol.

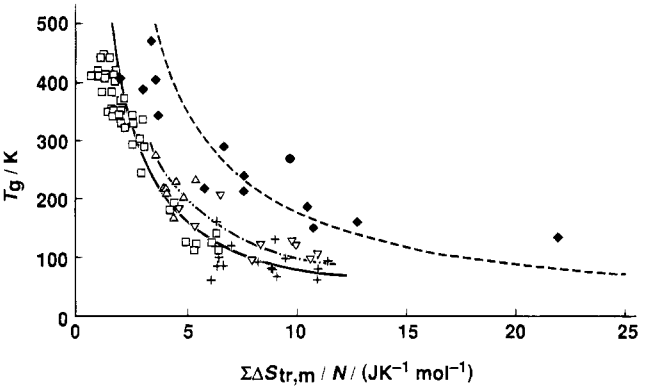

Figure 4. Relation between glass transition temperature (T_g) and transition–fusion entropies ($\Sigma\Delta S_{tr,m}/N$) for non(hydrogen-bonding) aromatic molecules (□), for mono(hydrogen-bonding) aromatic molecules (△), for non(hydrogen-bonding) aliphatic molecules (+), for mono(hydrogen-bonding) aliphatic molecules (▽), and for poly(hydrogen-bonding) compounds (♦). The curves indicate $T_g = h_g/(\Sigma\Delta S_{tr,m}/N)$ when h_g = 0.8 kJ/mol (—), when h_g = 1.0 kJ/mol (— · —), and when h_g = 1.8 kJ/mol (- - -). See Tables 2 and 3.

compounds. The T_g values for the aromatic and aliphatic molecules without a hydrogen-bonding site were almost on the solid correlation curve expressed by eq 7: $T_g = h_g/(\Sigma\Delta S_{tr,m}/N)$, where h_g was 0.8 kJ/mol. The T_g values for mono(hydrogen-bonding) molecules were somewhat higher than those for non(hydrogen-bonding) molecules without a site for the same $\Sigma\Delta S_{tr,m}/N$ values. The broken curve with h_g = 1.8 kJ/mol has been established for poly(hydrogen-bonding) molecules. The plots in a small $\Sigma\Delta S_{tr,m}/N$ region deviated from the theoretical curves to the small-T_g region because h_g decreased as predicted in the theoretical section. OXD-SA1 possesses three secondary amide hydrogen atoms. However, its plot was on the solid curves. This is probably due to intramolecular hydrogen-bond formation between the amide group and one of the oxdiazole nitrogen atoms.

Figure 5 shows the relations between T_g and $\Sigma\Delta S_{tr,m}/N$ for polymers. The data scattering was larger than that for the low molecular weight materials shown in Figure 4. One of the reasons is the difficulty in measuring the $\Sigma\Delta S_{tr,m}$ values. The data points for the polymers without hydrogen-bonding sites were located near the same solid curve in Figure 4. The plots for poly(hydrogen-bonding) polymers were above the curve as

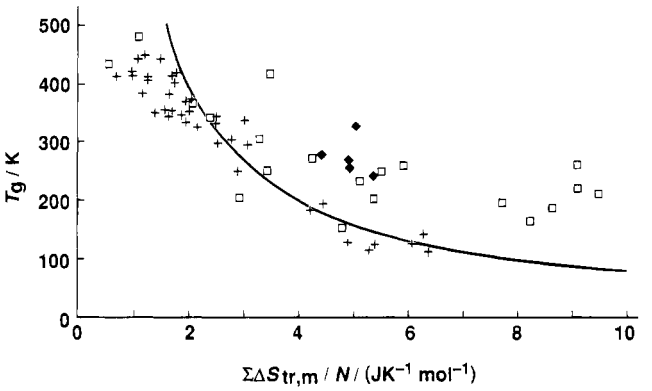

Figure 5. Relation between glass transition temperature (T_g) and transition–fusion entropies ($\Sigma\Delta S_{tr,m}/N$) for non(hydrogen-bonding) polymers (□), for poly(hydrogen-bonding) polymers (♦), for non(hydrogen-bonding) aromatic molecules (+). The solid curves indicate $T_g = h_g/(\Sigma\Delta S_{tr,m}/N)$ when h_g = 0.8 kJ/mol.

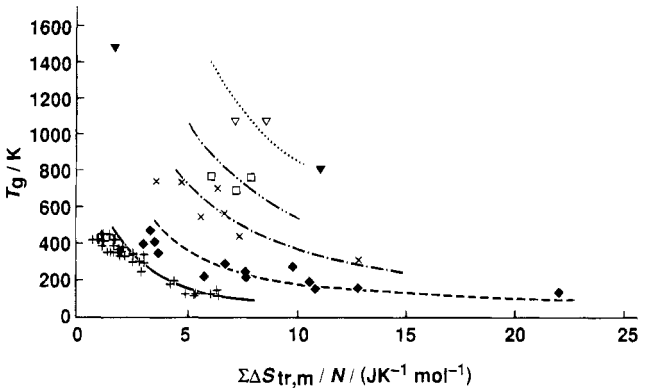

Figure 6. Relation between glass transition temperature (T_g) and transition–fusion entropies ($\Sigma\Delta S_{tr,m}/N$) for non(hydrogen-bonding) aromatic molecules (+), for poly(hydrogen-bonding) compounds (♦), for low network inorganic materials such as B_2O_3, P_2O_5, $M_2O{\cdot}SiO_2$ (×), for moderate network inorganic materials such as $M_2O{\cdot}2B_2O_3$ (□), for other moderate network inorganic materials such as $RO{\cdot}SiO_2$ (▽), and for high network inorganic materials such as SiO_2 and GeO_2 (▼). M and R mean an alkali metal and an alkali earth metal, respectively. The curves indicate $T_g = h_g/(\Sigma\Delta S_{tr,m}/N)$ when h_g = 0.8 kJ/mol (—), when h_g = 1.8 kJ/mol (- - -), when h_g = 3.5 kJ/mol (— · —), when h_g = 5.3 kJ/mol (— · · —), and when h_g = 8.3 kJ/mol (· · ·). See Table 6.

well as nonpolymeric molecules. However, non(hydrogen-bonding) polymers with large $\Sigma\Delta S_{tr,m}/N$ values were also located above the curve. This is probably caused by tangles in their flexible polymer chains, resulting in network formation. Sulfur is known to produce a glass composed of linear polymer chains. Sulfur could be classified as a linear polymer, as shown in Figure 5.

Figure 6 shows the relations between T_g and $\Sigma\Delta S_{tr,m}/N$ for various glass forming materials. The curves in the figure show eq 7: $T_g = h_g/(\Sigma\Delta S_{tr,m}/N)$. The ($h_g$/kJ mol^{-1}) value increased as the network degree increased in this order: non(hydrogen-bonding) aromatic and aliphatic compounds (0.8) < poly(hydrogen-bonding) compounds (1.8) < low network inorganic materials such as B_2O_3, P_2O_5, $M_2O{\cdot}SiO_2$ and selenium (3.5) < moderate network inorganic materials described by $M_2O{\cdot}2B_2O_3$ (5.3) < other moderate network inorganic materials such as $RO{\cdot}SiO_2$ ≈ high network inorganic materials such as SiO_2 and GeO_2 (8.3). M and R mean an alkali metal and an alkali earth metal, respectively. Selenium is known to yield a glass composed of linear polymer

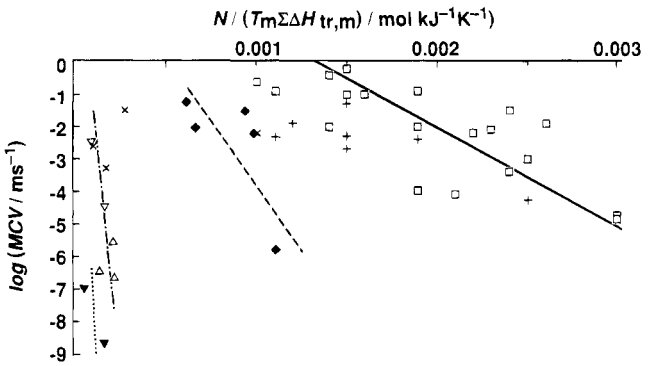

Figure 7. Relation between maximum crystal-growth velocity (MCV) and transition–fusion enthalpies $\{N/(T_m\Sigma\Delta H_{tr,m})\}$ for non(hydrogen-bonding) aromatic molecules (□), for mono(hydrogen-bonding) aromatic molecules (+), for poly(hydrogen-bonding) molecules (♦), for metals (×), for low network inorganic materials such as $M_2O{\cdot}SiO_2$ (△), for moderate network inorganic materials such as $M_2O{\cdot}2B_2O_3$ (▽), and for high network inorganic materials such as SiO_2 and GeO_2 (▼). M and R mean an alkali metal and an alkali earth metal, respectively. The straight lines indicate $MCV = k_0 \exp\{-h_{mc}N/(T_m\Sigma\Delta H_{tr,m})\}$ ($k_0 = 10^4$ m/s), when $h_{mc} = 6.9 \times 10^3$ K kJ/mol (—), when $h_{mc} = 1.7 \times 10^4$ K kJ/mol (- - -), when $h_{mc} = 1.2 \times 10^5$ K kJ/mol (— · —), when $h_{mc} = 2.4 \times 10^5$ K kJ/mol (· · ·). See Table 7.

chains as well as sulfur. However, some networks can be formed in selenium glass by interchain metallic bonding. The relatively small h_g value for high network materials is probably caused by the large D value in eq 6. The plots in a small $\Sigma\Delta S_{tr,m}/N$ region also deviated from the theoretical curves to a small-T_g region.

Maximum Crystal Growth Velocity (MCV). Table 7 indicates the numerical MCV data for various materials. Many data for non(hydrogen-bonding) aromatic compounds have been shown in a previous paper.[7]

Figure 7 shows the relations between MCV and $N/(T_m\Sigma\Delta H_{tr,m})$. MCV values are known to vary depending on the presence of impurities. Furthermore, MCV values are difficult to measure. In fact, MCV values which differ in order of magnitude have been reported by different researchers for the same materials. In the theoretical aspect, eq 9 was roughly estimated as described in the previous paper.[7] These are probably the main reasons for the data scattering in the figure.

As predicted in eq 12, $MCV = k_0 \exp\{-h_{mc}N/(T_m\Sigma\Delta H_{tr,m})\}$, the MCV values decreased as the $N/(T_m\Sigma\Delta H_{tr,m})$ value increased. The h_{mc} value increased as the network degree increased as well as h_g. The k_0 value was nearly constant (≈10^4 m/s). Among metals, only the plot for sodium was located in the region apart from the plots for other metals. This indicates that the network degree is not so large in alkali metal fusion.

Table 8 shows the crystallization data for high-T_g nonpolymeric organic compounds. The MCV and $T_{c,max}$ values have not been measured for molecules. The author roughly estimated their MCV value order by measuring ΔT_c ($=T_{c2} - T_{c1}$), as described in a previous paper.[7] T_{c1} and T_{c2} mean the crystallization temperatures observed when a glass is heated and when a fusion is cooled, respectively. Figure 8 shows the relations between ΔT_c and $N/(T_m\Sigma\Delta H_{tr,m})$. It is natural that the data scattering is wider than that in Figure 7, because a quantitative relation between ΔT_c and $N/(T_m\Sigma\Delta H_{tr,m})$ has not been obtained. Large $N/(T_m\Sigma\Delta H_{tr,m})$ values are preferable for small ΔT_c, i.e., small MCV. Poly(hydro-

Table 7. Relation between *MCV* and Transition–Fusion Enthalpies for Various Materials[a]

materials	T_m (K)	$T_{c,max}$ (K)	N	log(*MCV*) (m/s)	ref	$N/(T_m\Sigma\Delta H_{tr,m})$ (mol/(K kJ))
1,2,6-xylenol	319		9	−1.3	36	0.0015
1,2,3-xylenol	346		9	−1.9	36	0.0012
1,2,5-xylenol	348		9	−2.3	36	0.0011
1,3,5-xylenol	337		9	−2.3	36	0.0015
o-cresol	303	273	8	−2.4	36	0.0019
1,3,4-xylenol	334		9	−2.7	36	0.0015
phenyl salicylate	315	295	16	−4.3	36	0.0025
water	273	264	1	−1.2	37	0.00061
o-dihydroxybenzene	378	349	8	−1.5	36	0.00093
p-dihydroxybenzene	445	410	8	−2.0	36	0.00066
m-dihydroxybenzene	383	346	8	−2.2	36	0.00098
glycerol	292	270	6	−5.8	36	0.0011
tin	505		1	−1.5	36	0.00028
sodium	371	327	1	−2.2	36	0.001
aluminum	933	933	1	−2.6	36	0.0001
bismuth	545		1	−3.3	36	0.00017
$K_2O{\cdot}2SiO_2$		1210	9	−5.5	38	0.00021
$Li_2O{\cdot}2SiO_2$	1307	1130	9	−6.4	39	0.00013
$Na_2O{\cdot}2SiO_2$	1142	1050	9	−6.6	40	0.00022
$Li_2O{\cdot}2B_2O_3$	1190	1020	13	−2.5	41	0.00009
$Na_2O{\cdot}2B_2O_3$	1016	940	13	−4.5	41	0.00016
GeO_2	1388	1280	3	−7.0	42	0.00005
SiO_2 cristobalite	1996	1940	3	−8.7	43	0.00016

[a] Data for non(hydrogen-bonding) molecules were shown in a previous paper.[7]

Table 8. Crystallization Data[a] for Nonpolymeric Organic Compounds with High T_g

compound	T_m (K)	T_g (K)	T_{c1} (K)	T_{c2} (K)	ΔT_c (K)	$N/(T_m\Sigma\Delta H_{tr,m})$ (mol/(K kJ))
OXD-S1	446	412	n.o.[c]	n.o.	0	0.0060
OXD-B1	408	294	328	378	50	0.0024
TMTAA(OC_{14})[b]	398	336	357			0.0021
OXD-M1	423	303	n.o.	n.o.	0	0.0021
OXD-N1	453	290	325	410	85	0.0016
OXD-M0	412					0.0015
OXD-M3	451	294	349	n.o.	0	0.0018
OXD-M5	392	276	324	n.o.	0	0.0018
OXD-SA1	581	403	499	n.o.	0	0.0016
cholic acid	470	388	n.o.	n.o.	0	0.0015
methylandrostenediol	477	344	367	466	99	0.0012
TAAA	630	468	492			0.00075
BAAA	633	404	431			0.00071
CZ-S1		500	537			

[a] Data for non(hydrogen-bonding) aromatic molecules were shown in a previous paper.[7] [b] Reference 26. [c] Not obtained.

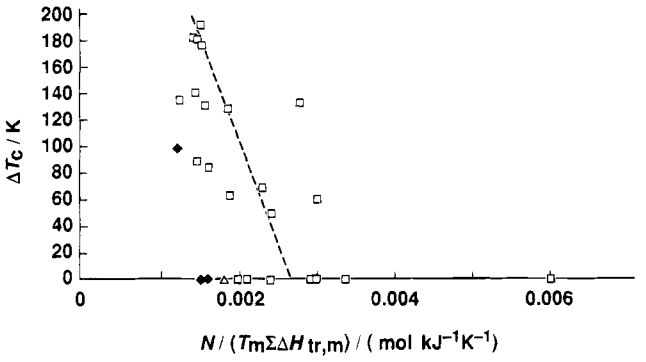

Figure 8. Relation between difference in crystallization temperatures (ΔT_c) and transition–fusion enthalpies $\{N/(T_m\Sigma\Delta H_{tr,m})\}$ for non(hydrogen-bonding) aromatic molecules (□), for mono(hydrogen-bonding) aromatic molecules (△), and for poly(hydrogen-bonding) molecules (♦).

gen-bonding) molecules indicate relatively small ΔT_c values for small $N/(T_m\Sigma\Delta H_{tr,m})$ values, the same as shown in Figure 7.

T_g and *MCV*. High glass-forming ability (i.e., low *MCV*) and high T_g are different things. Less-symmetric structures are suitable for decreasing *MCV* because of low T_m and small $\Sigma\Delta H_{tr,m}$ but are unsuitable for high T_g because of large $\Sigma\Delta S_{tr,m}$. Both symmetric and globular structures are necessary for high T_g and low *MCV*. These contents are described in detail in the previous paper.[7]

Synthesis of Poly(hydrogen-bonding) Aromatic Molecules with High T_g. According to eq 7, small $\Sigma\Delta S_{tr,m}$, large N, and large h_g are required for high-T_g nonpolymeric organic dyes. In a previous paper,[7] the molecular structures for small $\Sigma\Delta S_{tr,m}$ and large N have corresponded to large, symmetric, globular, rigid, and dense molecular structures with a small rotational moment by using the Hirshfelder–Stevenson–Eyring theory.[15] Large, symmetric, and globular structures are also preferable for increasing the $N/(T_m\Sigma\Delta H_{tr,m})$ values to produce stable glasses. According to this molecular design, the author and his colleague synthesized 10 1,3,4-oxadiazole derivatives with high T_g (381–442 K). The molecule with the highest T_g (473 K) in this material family (h_g = 0.8 kJ/mol) is considered to be *t*-Bu-TBATA reported by Shirota et al.[16] This molecule

(15) Hirschfelder, J. O.; Stevenson, D. P.; Eyring, H. *J. Chem. Phys.* **1937**, *5*, 896.
(16) Inada, H.; Shirota, Y. *Preprint of Annual Meeting of Chemical Society of Japan*, **1992**, *4F8 25*, p 997.
(17) Magill, J. H. *J. Chem. Phys.* **1967**, *47*, 2802.
(18) Mazurin, O. V.; Streltsina, M. V.; Shraiko-Shvaikovskaya, T. P. *Handbook of glass data, Part A*; Elsevier: Amsterdam, 1983; p 293.
(19) Reference 18, *Part A*, p 284.
(20) Reference 18, *Part B*, p 39.

has a globular structure with a very large N value (=118) and probably a small $\sum\Delta S_{tr,m}/N$ value.

The author has introduced plural secondary amide groups to increase h_g and has newly synthesized CZ-S1 and TAAA by a one-step condensation reaction. CZ-S1 and TAAA are large, symmetric, rigid, and dense molecules with plural sites for hydrogen bonding and have produced amorphous states with T_g as high as 500 and 468 K, respectively. CZ-S1 was not plotted in Figure 4 because it decomposed before melting. The CZ-S1 powder which was obtained by pouring its DMSO solution into water has been found to be amorphous by X-ray diffraction.

Conclusions

Quantitative relations between amorphous properties (T_g and MCV) and thermodynamic parameters (T_m, $\sum\Delta S_{tr,m}$, and $\sum\Delta H_{tr,m}$) have been established for various glass-forming materials. Network formation increases the activation energy for heavy atom rearrangement to raise T_g and to lower MCV. High-T_g nonpolymeric organic dye glasses can be formed from large, symmetric, globular, rigid, and dense molecules. Plural hydrogen-bonding sites increase T_g further.

Acknowledgment. The author thanks Dr. Ken Ando and Mr. Akira Miura of Toshiba R&D Center for enlightening discussions.

(21) Reference 18, *Part B*, p 642.
(22) Reference 18, *Part A*, p 496.
(23) Reference 18, *Part B*, p 124.
(24) Reference 18, *Part A*, p 79.
(25) Reference 18, *Part B*, p 369.
(26) McGregor, A. C.; Cryston, J. A. *Mol. Cryst. Liq. Cryst.* **1993**, *235*, 147. Temperature values were modified according to our DSC measurement method.[7]
(27) Privalko, V. P. *J. Phys. Chem.* **1980**, *84*, 3307.
(28) Sakka, S., Sakairo, T., Takahashi, K., Eds.; *Glass Handbook*; Asakura: Tokyo, 1975; p 868.
(29) Dean, J. A. Ed. *Lange's Handbook of Chemistry*, 12th ed.; McGraw-Hill: New York, 1978; pp 9-102–9-135.
(30) Reference 18, *Part A*, p 297.
(31) Reference 18, *Part A*, p 238.
(32) Reference 18, *Part A*, p 132.
(33) Reference 18, *Part A*, p 102.
(34) Reference 18, *Part A*, p 497.
(35) Lide, D. R. Ed. *Handbook of Chemistry and Physics*; CRC Press: Boca Raton, FL, 1993.
(36) Van Hook, A. *Crystallization*; Reinhold: New York, 1961; pp 166, 167.
(37) Reference 36, p 170.
(38) Reference 18, *Part A*, p 189.
(39) Reference 18, *Part A*, pp 203, 206.
(40) Reference 18, *Part A*, pp 190, 196.
(41) Reference 18, *Part B*, p 79.
(42) Reference 18, *Part B*, p 354.
(43) Reference 18, *Part A*, p 6.
(44) Moynihan, C. T. *J. Am. Ceram. Soc.* **1993**, *76*, 1081.